Archaeological Discovery, 2014, 2, 107-116
Published Online October 2014 in SciRes. http://www.scirp.org/journal/ad
http://dx.doi.org/10.4236/ad.2014.24012

Blackening of the Surfaces of Mesopotamian Clay Tablets Due to Manganese Precipitation

Etsuo Uchida*, **Ryota Watanabe**

Department of Resource and Environmental Engineering, Faculty of Science and Engineering, Waseda University, Tokyo, Japan
Email: *weuchida@waseda.jp

Received 10 August 2014; revised 8 September 2014; accepted 2 October 2014

Academic Editor: Dr. Xiuzhen Li, Emperor Qin Shihuang's Mausoleum Site Museum, China

Abstract

Blackening was observed on the surfaces of Mesopotamian clay tablets from Umma, Dilbat, Larsa, Ur, Babylon, Uruk, Sippar, and Nippur produced between the Third Dynasty of Ur and the Early Achaemenid Dynasty. Portable X-ray fluorescence analysis revealed that manganese was concentrated on the blackened surfaces. Rod-shaped materials with a length of 100 - 200 nm and a width of 30 nm were observed using a field emission scanning electron microscope. Distinct peaks were not necessarily obtained by micro-X-ray diffractometer analysis, but several samples of the black material showed peaks identifiable as buserite. These results may suggest that blackening on the surfaces of the clay tablets can be ascribed to the activity of manganese-oxidizing microbe. However, the size of the rod-shaped materials is too small compared to common bacteria.

Keywords

Clay Tablet, Mesopotamia, Maganese Concentration, Manganese-Oxidizing Microbe, Buserite

1. Introduction

Clay tablets were used as writing media in Mesopotamia, and cuneiform script was written on their surfaces. Clay tablets began to be used around 3300 BC; those made in the Third Dynasty of Ur, 2113-2006 BC, have been excavated most abundantly. The clay tablets record events related to agriculture, the economy, politics, and other matters.

In 2009, 2011, and 2012, the authors conducted non-destructive chemical analysis and magnetic susceptibility measurements on Mesopotamian clay tablets stored in the Yale Babylonian Collection of Yale University to

*Corresponding author.

How to cite this paper: Uchida, E., & Watanabe, R. (2014). Blackening of the Surfaces of Mesopotamian Clay Tablets Due to Manganese Precipitation. *Archaeological Discovery, 2,* 107-116. http://dx.doi.org/10.4236/ad.2014.24012

elucidate differences in the chemical composition between areas and the provenance of soil. Some of the results obtained in the investigation were published in Uchida et al. (2011) and Sterba et al. (2011). In the course of the study, the authors found blackening phenomena on the surfaces of the clay tablets. The blackened parts appear as spots or occupy wide areas. The blackening phenomena have previously been considered to be caused by soot attached on the surface during firing. However, chemical analysis using a portable X-ray fluorescence analyzer (pXRF) revealed that manganese is concentrated in the blackened parts. Blackening caused by manganese concentration on the surfaces of clay tablets has been reported previously (Laurito et al., 2005; Gütschow, 2012). However, the details of the formation mechanism have not yet been elucidated. Thus, in this study we focused on the blackening phenomena on the surfaces of the clay tablets and conducted a detailed study to determine the formation mechanism.

2. Methods

Non-destructive chemical analysis using an Innov-X Systems Delta Premium portable X-ray fluorescence analyzer (pXRF) with a Rh anode X-ray tube (4 W) was carried out on clay tablets showing blackening. The X-ray beam diameter is 9 mm. The test stand for the pXRF was used in the analysis. The measurement was conducted in "soil mode" using three different filters each for 20 sec (Beam 1 at 40 kV for U, Sr, Y, Zr, Th, Mo, Ag, Cd, Sn and Sb; Beam 2 at 40 kV for Fe, Co, Ni, Cu, Zn, W, Hg, As, Se, Pb, Bi and Rb; and Beam 3 at 15 kV for P, S, Cl, K, Ca, Ti, V, Cr, and Mn). The pXRF was calibrated in advance using 10 standard rock samples of the Geological Survey of Japan (JA-1, JA-2, JB-1b, JB-2, JB-3, JG-1a, JG-2, JGb-1, JR-1, and JR-2) (Imai et al., 1995). Calibration was conducted successfully for 17 elements: K (549), Ca (1389), Ti (65), V (16), Cr (14), Mn (73), Fe (264), Co (2), Ni (17), Cu (7), Zn (6), As (2), Rb (2), Sr (5), Y (1), Zr (2), and Pb (3). The figures in parentheses show standard deviations (ppm) of the chemical analysis in the average values of the clay tablets.

Samples for analyses were taken from blackened parts on the surfaces of clay tablets with no cuneiform script using a utility knife.

The chemical composition of the collected samples were determined using an electron probe X-ray microanalyzer (EPMA), which is composed of a JEOL JSM-6360 scanning electron microscope and an Oxford Instruments INCA ENERGY energy dispersive X-ray spectrometer. The accelerating voltage was 15 kV and the measuring time was fixed at 60 sec. The blackened parts of the clay tablets were analyzed using the EPMA; non-blackened parts were also analyzed as a control. The samples were coated with carbon. The chemical compositional information from the surface to a few μm in depth was obtained by the EPMA analysis in contrast to from the surface to a few mm in depth by the pXRF analysis.

Micro-X-ray diffraction analysis was conducted on the samples to identify the constituent minerals of the clay tablets and also the black materials. The analysis was conducted using a Rigaku RINT-RAPID micro-X-ray diffractometer (micro-XRD) with an X-ray tube with a Cu target. The tube current and voltage were 30 mA and 40 kV, and the measuring time was 30 min. A collimator with 100 μm ϕ was used in the measurement. The oscillating angles had a range of 7˚ - 14˚ for the ω axis (1˚/min) and −180˚ to +180˚ (6˚/min) for the ϕ axis.

Additionally, observations were conducted using a Hitachi S-4500S field emission scanning electron microscope (FE-SEM) on the samples taken from the black material of the clay tablets. The accelerating voltage was fixed at 15 kV. The samples were coated with platinum.

3. Blackening on the Surfaces of the Clay Tablets

The clay tablets investigated in this study are from Umma, Dilbat, Larsa, Ur, Babylon, Uruk, Sippar, and Nippur (**Figure 1**). The production periods of the studied tablets are from the Third Dynasty of Ur to the Early Achaemenid Dynasty (2113 BC to 330 BC). Economic or political events are described on the surfaces of the clay tablets.

The blackened parts caused by manganese precipitation occur as spots (NBC4846 and BCBT547), or as stains (NBC6240 and NBC30) (**Figure 2**). Occasionally a blackened part occupies a wide area on the surface of a clay tablet (NCBT2276 and YBC14659). Blackening is frequently observed on the surfaces of clay tablets, and more than 10% of clay tablets show blackening. The blackening phenomenon was seen on the tablets from all provenances investigated in this study. There is no correlation between the blackening phenomenon and the areas. It is considered that the black material was not formed in storage areas such as museums, but when the tablets were buried in soil.

The thickness of the black material on the surfaces of the clay tablets is less than 0.2 mm (**Figure 3**).

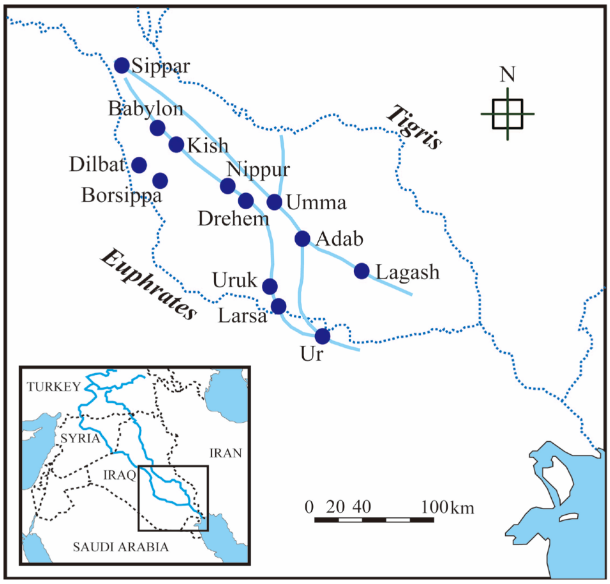

Figure 1. Map showing the provenance of the clay tablets investigated in this study, redrawn after Postgate (1992).

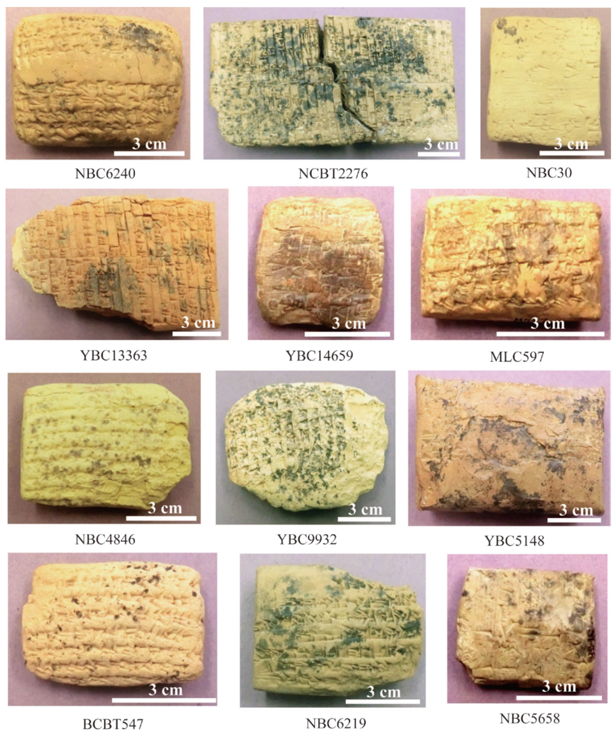

Figure 2. Clay tablets with blackened surfaces investigated in this study.

4. Results

4.1. Chemical Analysis Using pXRF

The results of the chemical analysis of the black material on the surfaces of the clay tablets using the pXRF are summarized in **Table 1**. Measurements were conducted on blackened surfaces and non-blackened surfaces of the clay tablets. As the surface is not completely covered by the black material even in the blackened part, and

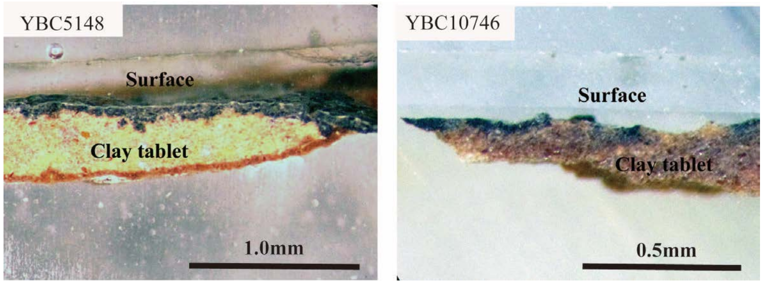

Figure 3. Cross-sections of the black material on the surfaces of clay tablets from Larsa (Old Babylonian period).

Table 1. Results of the chemical analysis of the black material and clay tablets using pXRF.

Area	Period	Sample no.		Ca	K	Ti	Cr	Mn	Fe	Co	Ni	Zn	As	Pb	Rb	Sr	Zr	Cu	V	Y
Umma	Ur III	YBC14659	Clay	124703	37277	3121	269	3212	39424	27	353	467	20	55	54.2	388	124	102	147	22.8
			Black part	90264	38577	3247	401	7913	37662	25	446	389	16	22	48.3	392	113	148	150	22.6
Dilbat	Early Neo-Babylonian	MLC597	Clay	105871	22461	4126	319	1510	48395	25	359	241	12	25	65.6	422	137	95	141	21.2
			Black part	111832	26923	4055	291	4397	50138	31	354	809	21	21	62.1	906	136	150	164	25.9
Larsa	Neo-Babylonian	NCBT547	Clay	108084	21290	3306	190	934	38865	24	284	199	8.1	16	53	309	114	1189	127	20.2
			Black part	130388	15467	3187	167	2613	38082	18	438	171	12	10	37.1	309	118	113	102	22.3
Ur	Ur III	NBC5658	Clay	97168	24951	3025	214	978	36155	18	262	71	13.1	12	52.9	302	109	49	104	17.6
			Black part	113470	23915	2732	174	4189	36059	23	462	85	11	24	54.6	331	111	48	113	20.2
Babylon	Neo-Babylonian	NBC4868	Clay	123245	14910	4307	261	987	51182	28	404	450	14	20	47.3	380	152	135	135	26.1
			Black part	128912	15593	4425	1226	4730	47792	23	3022	235	15	21	42.1	395	148	109	140	25.6
Babylon	Neo-Babylonian	NBC6219	Clay	100031	28441	3701	224	1619	45576	26	311	260	12	34	58.3	379	124	450	123	23.8
			Black part	87265	29976	3967	236	10203	43361	12	616	171	15	25	52.6	361	125	104	174	20.4
Uruk	Neo-Babylonian	YBC9932	Clay	126915	12135	3825	131	1283	46025	26	392	218	17	10	35.5	299	124	68	122	22.5
			Black part	129335	15354	3641	184	9171	44830	20	741	389	17	-	35.5	346	130	90	160	24.6
Umma	Ur III	NCBT2276	Clay	114890	18394	2306	156	797	26948	20.6	228	58	10.6	16	51.9	246	94	36	77	15.8
			Black part	86184	19079	2790	160	13588	32707	21	868	80	14	27	51.1	270	93	55	154	19.2
Larsa	Old-Babylonian	YBC5148	Clay	84619	36260	3463	245	1140	38444	24	260	90	9.7	18	55.9	361	109	76	116	18.2
			Black part	98000	21457	3058	203	21996	35638	10	501	114	21	47	50	322	108	113	263	20.5
Umma	Ur III	YBC13363	Clay	31799	65720	4916	1863	993	55408	25	784	156	22	73	90	231	129	92	195	24
			Black part	52286	50108	4409	1317	20275	51628	18	844	142	23	40	81	265	127	68	259	23.5
Sippar	Early Achae-menid	NBC6240	Clay	110706	27767	3878	233	4060	43090	19	370	456	18	43	50.7	374	122	266	121	22.4
			Black part	86802	26993	4233	257	11806	43924	11	507	290	9	33	50	356	124	189	128	21.1
Nippur	Ur III	NBC30	Clay	125944	36130	3837	462	1685	43057	18	367	409	13	20	51.1	559	131	103	191	23.6
			Black part	100134	51106	4172	469	14551	45858	27	946	438	10	22	62.3	580	140	128	133	22.1

also the black material is thin (less than 0.2 mm in thickness) (**Figure 3**), it is certain that there is some contribution from the clay itself to the analytical results.

Figure 4 shows the ratio of the chemical composition of the blackened part to that of non-blackened part of the clay tablets. The results show that manganese is concentrated in the blackened parts 2 - 20 times more than in the non-blackened parts. Next to manganese, nickel is concentrated in the blackened parts (1 - 7 times). Although not present in every tablet, vanadium, chromium, zinc, arsenic, and lead are concentrated in the blackened parts.

4.2. Chemical Analysis Using EPMA

EPMA analysis was conducted on four clay tablets: NBC6219, NBC30, BCBT2276, and YBC5148. We analyzed black material on the surfaces of the clay tablets and also the clay itself for comparison. The analysis was carried out at three points on the black material and at three points on the clay for each sample. The results are summarized in **Table 2**, and the points analyzed are shown in **Figure 5**. In the calculation, Mn was treated as Mn^{4+} and Fe as Fe^{3+}.

The EPMA analysis reflects the chemical composition in shallower parts of the tablets than the pXRF analysis does. Therefore, the EPMA analysis gives us more accurate information on the chemical composition of the black material. However, EPMA is not suitable for analysis of minor elements because of its low sensitivity.

The results show that that manganese is concentrated in the black material 20 - 240 times more than in the original clay tablets. For Fe, the content is low in the black material compared with the original clay tablet. Therefore, it is considered that the black material is composed essentially of manganese. Although Si, Al, Mg, and K were also detected in the black material, these elements are considered to be derived from the minerals making up the clay tablets. A few percent of S was detected in the black material, but the S content in the clay tablets (non-black material) is usually less than 1%. This fact suggests that S is concentrated more or less in the black material. The Ca content is also high in the black material, and so it is considered that gypsum ($CaSO_4 \cdot 2H_2O$) exists in the black material. In clay tablets NBC6219, NBC30, and YBC5148, a considerable amount of Ca compared with S is contained in the black material. This may suggest that Ca is present in calcite as well as in gypsum.

4.3. Micro-XRD Analysis

Table 3 summarizes the constituent minerals of the clay tablets, identified using micro-XRD. Quartz and calcite are identified from all clay tablets. Dolomite is found in several clay tablets, as is gypsum. However, it is consi-

Figure 4. Concentration of each element in the black material on the surface of the clay tablets compared with that in the clay tablets, analyzed by the EPMA.

Table 2. Results of the chemical analysis of the black material and clay tablets using the EPMA. The totals were normalized to 100%.

	NBC6219						NBC30					
	Black-1	Black-2	Black-3	Clay-1	Clay-2	Clay-3	Black-1	Black-2	Black-3	Clay-1	Clay-2	Clay-3
Na	0.58	0.47	0.62	0.88	1.13	1.09	0.58	0.41	0.28	1.67	0.96	1.37
Mg	2.89	2.82	3.05	4.89	4.93	4.50	2.85	2.94	2.35	3.63	3.39	2.89
Al	4.43	4.49	4.84	8.72	8.17	7.82	3.09	3.44	4.98	6.93	7.02	11.15
Si	13.70	13.74	14.33	25.10	24.61	23.41	8.69	6.80	6.51	21.33	23.99	21.96
S	3.60	4.84	4.59	0.12	0.90	0.07	1.64	3.15	4.11	0.03	0.04	0.03
Cl	0.12	0.33	0.23	0.16	0.17	0.12	2.08	3.05	4.29	0.62	0.23	0.14
K	1.61	1.64	1.52	2.67	2.13	2.35	0.60	0.23	0.46	1.95	4.10	7.03
Ca	12.67	9.51	10.29	3.76	5.81	9.44	22.22	25.59	27.40	15.22	9.89	5.24
Mn	13.06	13.75	10.79	0.21	0.14	0.27	17.30	13.96	7.98	0.20	0.13	0.34
Fe	5.09	5.15	6.52	7.87	6.21	6.62	3.30	3.09	4.41	5.84	6.43	6.13
O	42.23	43.26	43.23	45.61	45.79	44.32	37.66	37.33	37.22	42.58	43.82	43.72
Total	100	100	100	100	100	100	100	100	100	100	100	100
	BCBT2276						YBC5148					
	Black-1	Black-2	Black-3	Clay-1	Clay-2	Clay-3	Black-1	Black-2	Black-3	Clay-1	Clay-2	Clay-3
Na	0.51	0.48	0.62	1.20	0.50	0.30	3.16	0.40	1.75	1.28	0.96	1.45
Mg	4.75	4.97	5.40	4.36	3.96	4.59	4.68	5.10	3.08	4.59	4.66	3.65
Al	6.88	6.38	6.88	7.62	6.96	6.34	3.45	4.70	1.87	7.72	8.74	6.32
Si	22.29	18.36	19.15	24.28	19.87	19.65	7.38	14.32	3.92	21.35	23.72	26.95
S	0.11	1.99	1.36	0.64	0.02	0.39	3.97	4.02	11.56	0.08	0.09	0.08
Cl	1.05	3.29	2.66	0.33	0.47	0.43	4.40	1.02	1.74	0.98	0.39	1.18
K	2.25	1.59	1.81	1.94	2.44	2.10	1.07	1.33	0.59	2.19	2.64	1.83
Ca	8.26	10.43	10.47	9.42	8.17	17.57	11.61	15.03	15.12	12.74	8.47	7.63
Mn	4.68	5.62	4.36	0.05	0.25	0.07	19.59	6.75	16.89	0.08	0.10	0.19
Fe	5.43	4.28	4.52	5.11	5.39	6.52	1.99	4.96	0.98	6.04	5.55	5.48
O	43.79	42.61	42.77	45.06	51.95	42.03	38.71	42.35	42.49	42.95	44.69	45.24
Total	100	100	100	100	100	100	100	100	100	100	100	100

Table 3. Constituent minerals of the clay tablets identified using a micro X-ray diffractometer.

Area	Period	Sample no.	Quartz	Calcite	Pyroxene	Gypsum	Dolomite	Plagioclase	Buserite
Umma	Ur III	YBC14659	++	+		+		+	
Dilbat	Early Neo-Babylonian	MLC597	++	+				+	
Larsa	Neo-Babylonian	NCBT547	++	++			++		
Ur	Ur III	NBC5658	++	++	+	+	+	+	
Babylon	Neo-Babylonian	NBC4846	++	+			++	+	
Babylon	Neo-Babylonian	NBC6219	++	++		+		+	
Uruk	Neo-Babylonian	YBC9932	++	++		+		+	
Umma	Ur III	NCBT2276	++	++		+	+		+
Larsa	Old-Babylonian	YBC5148	++	+		+	+		+
Umma	Ur III	YBC13363	++	+					
Sippar	Early Achaemenid	NBC6240	++	++			+	+	
Nippur	Ur III	NBC30	++	++		+			+

Note: ++: a large amount; +: a small amount.

dered that gypsum was formed on the surface of the clay tablets when they were buried in soil. Additionally, small amounts of plagioclase and pyroxene were identified from some clay tablets.

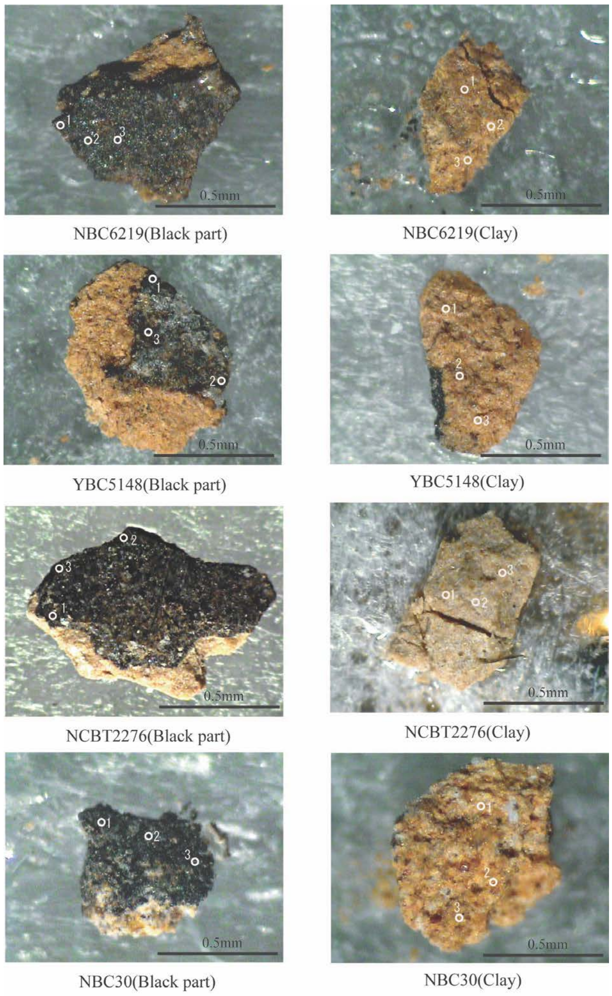

Figure 5. Photographs showing the points analyzed by the EPMA.

In the micro-XRD analysis, a 10 Å manganese mineral was detected in the black material of clay tablets YBC5148, NBC30, and NCBT2276 (**Figure 6**). Although a large amount of manganese was present in the black material, XRD peaks attributable to manganese minerals were not necessarily obtained from all the clay tablets. This fact may suggest that manganese exists as amorphous materials. Buserite and todorokite are the candidates for 10 Å manganese minerals. To identify them, samples with black material were placed in an oven at 105˚C for 24 h, and were measured with the micro-XRD. As a result, birnessite newly appeared instead of the 10 Å manganese mineral. This suggests that the 10 Å manganese mineral in the black material is not todorokite, but buserite (Sato et al., 2000). Buserite is known to be a major constituent mineral of manganese nodules on the sea floor (Burns et al., 1983; Giovanoli et al., 1971; Usui & Someya, 1997). The participation of manganese-oxidizing bacteria in the formation of manganese nodules was pointed out by LaRock and Ehrlich (1975), Thiel (1925), and Wang and Müller (2009). Gypsum ($CaSO_4 \cdot 2H_2O$) was changed into bassanite ($CaSO_4 \cdot 1/2H_2O$) by dehydration when the samples were dried at 105˚C.

4.4. FE-SEM Observations

Rod-shaped materials with a length of 100 - 200 nm and a width of 30 nm were observed on the blackened surfaces of the clay tablets by the FE-SEM. Platy manganese-bearing crystals were also seen. It appears that rod-shaped materials were gathered and changed into platy crystals (**Figure 7**). This may suggest that platy manganese-bearing minerals were formed by recrystallization of the remains of the manganese-oxidizing mi-

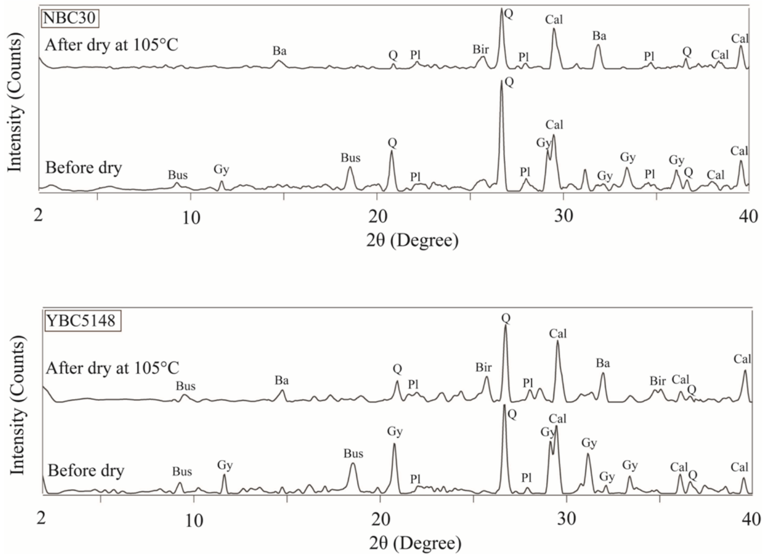

Figure 6. X-ray diffraction patterns of the black material taken from clay tablets NBC30 and YBC5148, obtained using the micro-X-ray diffractometer. Abbreviations: Q, quartz; Pl, plagioclase; Cal, calcite; Gy, gypsum; Ba, bassanite; Bir, birnessite; and Bus, buserite.

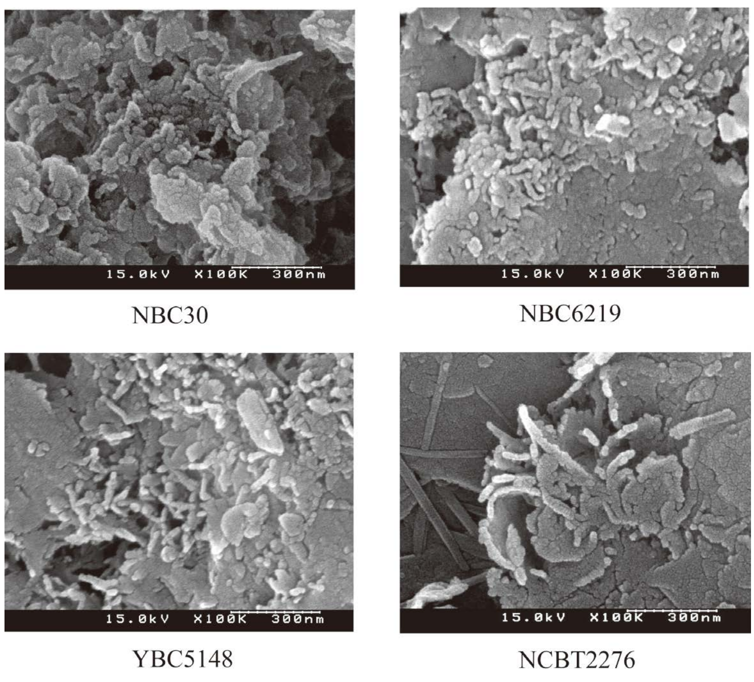

Figure 7. FE-SEM images of the black material on the surfaces of the clay tablets.

crobe. However, the size of the rod-shaped materials is too small compared with common bacteria.

5. Conclusion

The pXRF and EPMA analyses revealed that the black material on the surfaces of the Mesopotamian clay tablets is mainly composed of manganese. As XRD peaks attributable to manganese minerals were not obtained from all samples by micro-XRD analysis, it seems that the manganese-bearing material is mainly present as amorphous manganese oxide or hydroxide. However, XRD peaks identifiable as buserite were obtained from some samples. Additionally, under the FE-SEM, rod-shaped bacteria (bacilli)-like materials with a length of 100 - 200 nm and a width of 30 nm were seen, which were gathered and changed into platy crystals. These facts may suggest that the blackening phenomena on the surfaces of the clay tablets were caused by the action of manganese-oxidizing microbe. Oxidation and concentration of manganese by microbial activity are also seen in manganese nodules and crusts on the sea floor and in desert varnish on the rock surface (Dorn & Oberlander, 1981; Perry & Adams, 1978; Potter & Rossman, 1977; Wang et al., 2011). Similar phenomena of manganese concentration by the microbial activity are observed in caves and the bottoms of rivers (Kanai et al., 2006). Concentration of manganese or iron by microbial activity is frequently seen in the natural world. However, the size of manganese-oxidizing microbe-like materials observed in this study by FE-SEM is one order of magnitude smaller than the manganese-oxidizing microbe found in manganese nodules and desert varnish reported previously (Wang & Müller, 2009; Dorn & Oberlander, 1981; Wang et al., 2011). To characterize and identify the microbe-like materials seen in the clay tablets, DNA analysis (16S rDNA) will be indispensable in future studies in spite of difficulty in collecting the sufficient amount of sample.

Acknowledgements

Clay tablets stored in the Yale Babylonian Collection of Yale University were studied in this investigation. We would like to express our sincere thanks to Prof. B. Foster for permission to access to the Yale Babylonian Collection. During the investigation at Yale University, Dr. U. Kasten and Dr. E. Payne kindly helped us. Dr. C. E. Watanabe of Osaka Gakuin University arranged the investigation at Yale University. We would like to thank them for their useful help. This study was financially supported in part by a Grant-in-Aid for Scientific Research of the Japan Society for the Promotion of Science (Grant no. 23310190: C. E. Watanabe).

References

Burns, R. G., Burns, V. M., & Stockman, H. W. (1983). A Review of the Todorokite-Buserite Problem: Implications to the Mineralogy of Marine Manganese Nodules. *American Mineralogists, 68,* 972-980.

Dorn, R. I., & Oberlander, T. M. (1981). Microbial Origin of Desert Varnish. *Science, 213,* 1245-1247. http://dx.doi.org/10.1126/science.213.4513.1245

Giovanoli, R., Feitknecht, W., & Fischer, F. (1971). Uber Oxidhydroxide des vierwertigen Mangans mit Schichtengitter, 3. Mitteilung: Reduktion von Mangan (Ill)-manganat (IV) mit Zimtalkohol. *Helvetica Chimica Acta, 54,* 1112-1124. http://dx.doi.org/10.1002/hlca.19710540421

Gütschow, C. (2012). Methoden zur Restaurierung von ungebrannten und gebrannten Keilschrifttafeln—Gestern und Heute. In *Berliner Beiträge zum Vorderen Orient Band 22,* PeWe-Verlag, Gladbeck.

Imai, N., Terashima, S., Itoh, S., & Ando, A. (1995). 1994 Compilation Values for GSJ Reference Samples, "Igneous Rock Series". *Geochemical Journal, 29,* 91-95. http://dx.doi.org/10.2343/geochemj.29.91

Kanai, Y., Mita, N., Takeuchi, R., Yoshida, S., & Kuchitsu, N. (2006) Study on Characterization of Manganese-Oxidizing Bacteria in the Natural Environment and Estimation of Its Effect. *Bulletin of the Geological Survey of Japan, 57,* 1-15. (in Japanese)

LaRock, P. A., & Ehrlich, H. L. (1975). Observations of Bacterial Microcolonies on the Surface of Ferromanganese Nodules from Blake Plateau by Scanning Electron Microscopy. *Microbiology Ecology, 2,* 84-96. http://dx.doi.org/10.1007/BF02010383

Laurito, R., Mezzasalma, A., & Verderrame, L. (2005). Text and Labels: A Case Study from Neo-Sumerian Umma. In R. Biggs, J. Myers, & M. T. Roth (Eds.), *Proceedings of the 51st Rencontre Assyriologique International* (pp. 99-110). Chicago: Oriental Institute of the University of Chicago.

Perry, R. S., & Adams, J. B. (1978). Desert Varnish: Evidence for Cyclic Deposition of Manganese. *Nature, 276,* 489-491. http://dx.doi.org/10.1038/276489a0

Potter, R. M., & Rossman, G. R. (1977). Desert Varnish: The Importance of Clay Minerals. *Science, 196,* 1446-1448. http://dx.doi.org/10.1126/science.196.4297.1446

Sato, Y., Hayashi, J., Nishimori, M., Ono, S., & Takematsu, N. (2000). Manganese Oxide Minerals Formed by Microbial Mediation. *Oceanography in Japan, 9,* 193-204. (in Japanese) http://dx.doi.org/10.5928/kaiyou.9.193

Sterba, J. H., Uchida, E., Bichler, M., Sasaki, T., & Watanabe, C. (2011). NAA and XRF Analyses and Magnetic Susuceptibility Measurement. *Scienze dell'antichita, 17,* 409-426.

Thiel, G. A. (1925). Manganese Precipitated by Microorganisms. *Economic Geology, 20,* 301-310. http://dx.doi.org/10.2113/gsecongeo.20.4.301

Uchida, E., Sasaki, T., & Watanabe, C. (2011). Non-Destructive Analyses Applied to Mesopotamian Clay Tablets. *Scienze dell'antichita, 17,* 343-401.

Usui, A., & Someya, M. (1997). Distribution and Composition of Marine Hydrogenetic and Hydrothermal Manganese Deposits in the Northwest Pacific. In K. Nicholson, J. R. Hein, B. Bühn, & S. Dasgupta (Eds.), *Manganese Mineralization: Geochemistry and Mineralogy of Terrestrial and Marine Deposits* (pp.177-198). London: Geological Society of London Special Publication No. 119.

Wang, W., & Müller, W. E. G. (2009). Marine Biominerals: Perspectives and Challenges for Polymetallic Nodules and Crusts. *Trends in Biotechnology, 27,* 375-383. http://dx.doi.org/10.1016/j.tibtech.2009.03.004

Wang, X., Zeng, L., Wiens, M., Schloßmacher, U., Jochum, K. P., Schröder, H. C., & Müller, W. E. G. (2011). Evidence for a Biogenic, Microorganismal Origin of Rock Varnish from the Gangdese Belt of Tibet. *Micron, 42,* 401-411. http://dx.doi.org/10.1016/j.micron.2010.12.001